Spectrochimica Acta Part A: Molecular and Biomolecular Spectroscopy 125 (2014) 404–413

Contents lists available at ScienceDirect

Spectrochimica Acta Part A: Molecular and Biomolecular Spectroscopy

journal homepage: www.elsevier.com/locate/saa

Exploring DNA binding and nucleolytic activity of few 4-aminoantipyrine based amino acid Schiff base complexes: A comparative approach

N. Raman *, A. Sakthivel, N. Pravin

Research Department of Chemistry, VHNSN College, Virudhunagar 626 001, Tamil Nadu, India

HIGHLIGHTS

- Designing and synthesis of effective chemical nucleases.
- 4-Aminoantipyrine based metal complexes are superior DNA binding agents.
- Valine Schiff base complexes are better intercalators.
- Synthesis of better antimicrobial agents against pathogens.

GRAPHICAL ABSTRACT

4-Aminoantipyrine derived Schiff bases and their metal complexes are valuable in designing novel agents for targeting nucleic acids as well as setting the stage for the synthesis of chemical anticarcinogenic drugs.

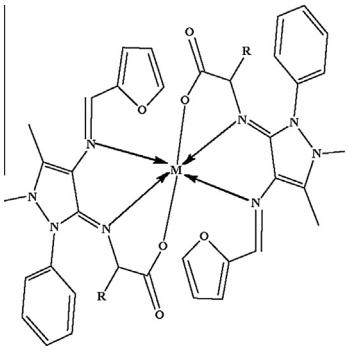

ARTICLE INFO

Article history:
Received 28 October 2013
Received in revised form 20 January 2014
Accepted 22 January 2014
Available online 6 February 2014

Keywords:
4-Aminoantipyrine
Schiff-base complexes
Calf thymus DNA
Antimicrobial studies
Intercalative mode

ABSTRACT

A series of novel Co(II), Cu(II), Ni(II) and Zn(II) complexes were synthesized from Schiff base(s), obtained by the condensation of 4-aminoantipyrine with furfural and amino acid (glycine(L1)/alanine(L2)/valine(L3)) and respective metal(II) chloride. Their structural features and other properties were explored from the analytical and spectral methods. The binding behaviors of the complexes to calf thymus DNA were investigated by absorption spectra, viscosity measurements and cyclic voltammetry. The intrinsic binding constants for the above synthesized complexes are found to be in the order of 10^2 to 10^5 indicating that most of the synthesized complexes are good intercalators. The binding constant values (K_b) clearly indicate that valine Schiff-base complexes have more intercalating ability than alanine and glycine Schiff-base complexes. The results indicate that the complexes bind to DNA through intercalation and act as efficient cleaving agents. The *in vitro* antibacterial and antifungal assay indicates that these complexes are good antimicrobial agents against various pathogens. The IC_{50} values of $[Ni(L1)_2]$ and $[Zn(L1)_2]$ complexes imply that these complexes have preferable ability to scavenge hydroxyl radical.

* Corresponding author. Tel.: +91 092451 65958; fax: +91 4562 281338.
E-mail address: ramchem1964@gmail.com (N. Raman).

http://dx.doi.org/10.1016/j.saa.2014.01.108
1386-1425/

Introduction

The increasing microbial resistance to antibiotics is a very important necessity which inculcates the search for new compounds with potential effects against pathogenic bacteria and fungi [1,2]. The most spectacular advances in medicinal chemistry have been made when heterocyclic compounds played an important role in regulating biological activities. Heterocyclic moieties can be found in a large number of compounds which display biological activity [3]. Antipyrine (N-heterocyclic compound) and its derivatives exhibit a wide range of biological activities and applications. Because of their interesting structural features as well as the biological activity, a wide range of metal complexes derived from antipyrine derivatives have been reported [4,5]. Pyrazolone-based ligands display variable complexing behavior and a variety of coordination possibilities to metal centers.

The coordination chemistry of Schiff base complexes involving oxygen and nitrogen donor ligands has excited great interest among chemists in recent years due to their applications in catalysis and their relevance to bio-inorganic systems [6]. Inorganic complexes can be used in foot-printing studies, as sequence specific DNA binding agents, as diagnostic agents in medicinal applications, and for genomic research. A large number of metal complexes have been used as cleavage agents for DNA and also for novel potential DNA-targeted antitumor drugs. This is essential for further expected applications in many areas like biological and medicinal significance as potential artificial gene regulators (or) cancer chemotherapeutic agents [7].

In view of biological importance of Schiff base derived from the condensation of 4-aminoantipyrine with furfural and amino acids (glycine/alanine/valine), its applications in various fields, in the present investigation it is thought to synthesize the metal complexes with transition metal ions such as Co(II), Ni(II), Cu(II) and Zn(II). It is therefore of interest to carryout investigations to understand how a ligand environment could affect the redox properties of the central metal and thereby the spectral properties and also interested to explore the DNA binding and DNA cleavage activity of synthesized complexes. This result would be helpful for understanding the binding mode of the complex to DNA and it also lays a foundation for developing new useful DNA probes and effective inorganic complex nucleases.

Experimental

Reagents and instruments

All reagents, 4-aminoantipyrine, furfural, glycine, alanine, valine and metal(II) chlorides were of Merck products and they were used as supplied. Commercial solvents were distilled and then used for the preparation of ligands and their complexes. DNA was purchased from Bangalore Genei (India). Microanalyses (C, H and N) were performed in Carlo Erba 1108 analyzer at Sophisticated Analytical Instrument Facility (SAIF), Central Drug Research Institute (CDRI), Lucknow, India. Molar conductivities in DMF (10^{-3} M) at room temperature were measured by using Systronic model-304 digital conductivity meter. Magnetic susceptibility measurement of the complexes was carried out by Gouy balance using copper sulfate pentahydrate as the calibrant. Infrared spectra (4000–350 cm^{-1} KBr disc) of the samples were recorded on an IR Affinity-1 FT-IR Shimadzu spectrophotometer. NMR spectra were recorded on a Bruker Avance Dry 300 FT-NMR spectrometer in $CDCl_3$, using TMS as the internal reference. Mass spectrometry experiments were performed on a JEOL-AccuTOF JMS-T100LC mass spectrometer equipped with a custom-made electrospray interface (ESI). EPR spectra were recorded on a Varian E 112 EPR spectrometer in DMSO solution both at room temperature (300 K) and liquid nitrogen temperature (77 K) using TCNE (tetracyanoethylene) as the g-marker. The absorption spectra were recorded by using Shimadzu model UV-1601 spectrophotometer at room temperature.

Synthesis of Schiff base ligands

An ethanolic solution of 4-aminoantipyrine (0.02 M) was added to an ethanolic solution of furfural (0.02 mol) and amino acid (glycine (**L1**)/alanine (**L2**)/valine **(L2**) (0.02 M)) which was dissolved in alcoholic potash. The resultant mixture was refluxed for 4 h. The solid product formed was filtered and recrystallized from ethanol.

L1. Yield: 74%. M.F. $C_{18}H_{17}N_4O_3$. IR (KBr pellet, cm^{-1}): 1652 ν(—C=N); 1602 ν(—HC=N); 3435, 1427, 1390 ν((—COO^-), (—COO^-) ν_{asy}, (—COO^-) ν_{sy}). ^1H NMR (δ): (aromatic) 6.6–7.1 (m); (COOH) 11(s); (C—CH_3) 2.3 (s); (N—CH3) 3.1(s); (CH=N) 9.3(s). MS *m*/*z* (%): 338 $[M + 1]^+$. λ_{max} (cm^{-1}) in DMF, 29,240, 37,075.

L2. Yield: 70%. M.F. $C_{19}H_{19}N_4O_3$. IR (KBr pellet, cm^{-1}): 1650 ν(—C=N); 1602 ν(—HC=N); 3431, 1427, 1389 ν((—COO^-), (—COO^-) ν_{asy}, (—COO^-) ν_{sy}). ^1H NMR (δ): (aromatic) 6.6–7.4 (m); (COOH) 11(s); (C—CH_3) 2.4 (s); (N—CH_3) 3.3 (s); (CH=N) 9.3(s). MS *m*/*z* (%): 352 $[M + 1]^+$. λ_{max} (cm^{-1}) in DMF, 29,411, 35,335.

L3. Yield: 76%. M.F. $C_{21}H_{23}N_4O_3$. IR (KBr pellet, cm^{-1}): 1652 ν(—C=N); 1602 ν(—HC=N); 3441, 1419, 1390 ν((—COO^-), (—COO^-) ν_{asy}, (—COO^-) ν_{sy}). ^1H NMR (δ): (aromatic) 6.5–7.3 (m); (COOH) 11(s); (C—CH_3) 2.3 (s); (N—CH_3) 3.2 (s); (CH=N) 9.3(s). MS *m*/*z* (%): 380 $[M + 1]^+$. λ_{max} (cm^{-1}) in DMF, 29,450, 35,575.

Synthesis of metal complexes

A solution of metal(II) chloride in ethanol (0.02 M) was mixed with an ethanolic solution of the Schiff base (0.04 M), and the resultant mixture was refluxed for 3 h. The solid complex precipitated was filtered off and washed thoroughly with ethanol and petroleum ether and dried over anhydrous $CaCl_2$ under vacuum. Schematic diagram for the synthesis of ligand and metal complexes is given in Scheme 1.

$[Cu(L1)_2]$. Yield: 69%. M.F. $C_{36}H_{34}N_8O_6Cu$. IR (KBr pellet, cm^{-1}): 1647 ν(—C=N); 1593 ν(—HC=N); 3417, 1417, 1379 ν((—COO^-), (—COO^-) ν_{asy}, (—COO^-) ν_{sy}); 501 ν(M—O); 449 ν(M—N). MS *m*/*z* (%): 739 $[M + 1]^+$. λ_{max} (cm^{-1}) in DMF, 11,050, 37,453.

$[Cu(L2)_2]$. Yield: 72%. M.F.$C_{38}H_{38}N_8O_6Cu$. IR (KBr pellet, cm^{-1}): 1645 ν(—C=N); 1593 ν(—HC=N); 3429, 1419, 1378 ν((—COO^-), (—COO^-) ν_{asy}, (—COO^-) ν_{sy}); 500 ν(M—O); 435 ν(M—N). MS *m*/*z* (%): 767 $[M + 1]^+$. λ_{max} (cm^{-1}) in DMF, 11,049, 37,878.

$[Cu(L3)_2]$. Yield: 68%. M.F. $C_{42}H_{46}N_8O_6Cu$. IR (KBr pellet, cm^{-1}): 1647 ν(—C=N); 1593 ν(—HC=N); 3417, 1417, 1379 ν((—COO^-), (—COO^-) ν_{asy}, (—COO^-) ν_{sy}); 501 ν(M—O); 449 ν(M—N). MS *m*/*z* (%): 823 $[M + 1]^+$. λ_{max} (cm^{-1}) in DMF, 12,254, 29,586.

$[Co(L1)_2]$. Yield: 63%. M.F. $C_{36}H_{34}N_8O_6Co$. IR (KBr pellet, cm^{-1}): 1645 ν(—C=N); 1593 ν(—HC=N); 3408, 1415, 1380 ν((—COO^-), (—COO^-) ν_{asy}, (—COO^-) ν_{sy}); 503 ν(M—O); 437 ν(M—N). MS *m*/*z* (%): 734 $[M + 1]^+$. λ_{max} (cm^{-1}) in DMF, 11,025, 14,903, 29,280.

$[Co(L2)_2]$. Yield: 83%. M.F. $C_{38}H_{38}N_8O_6Co$. IR (KBr pellet, cm^{-1}): 1645 ν(—C=N); 1597 ν(—HC=N); 3429, 1419, 1382 ν((—COO^-), (—COO^-) ν_{asy}, (—COO^-) ν_{sy}); 500 ν(M—O); 428 ν(M—N). MS *m*/*z* (%): 914 $[M + 1]^+$. λ_{max} (cm^{-1}) in DMF, 12,150, 13,774, 29,325.

$[Co(L3)_2]$. Yield: 78%. M.F. $C_{42}H_{46}N_8O_6Co$. IR (KBr pellet, cm^{-1}): 1647 ν(—C=N); 1597 ν(—HC=N); 1417, 1379 ν((—COO^-) ν_{asy}, (—COO^-) ν_{sy}); 570 ν(M—O); 435 ν(M—N). MS *m*/*z* (%): 818 $[M + 1]^+$. λ_{max} (cm^{-1}) in DMF, 11,049, 12,500, 29,761.

$[Ni(L1)_2]$. Yield: 59%. M.F. $C_{36}H_{34}N_8O_6Ni$. IR (KBr pellet, cm^{-1}): 1645 ν(—C=N); 1591 ν(—HC=N); 3410, 1409, 1382 ν((—COO^-), (—COO^-) ν_{asy}, (—COO^-) ν_{sy}); 503 ν(M—O); 433 ν(M—N). MS *m*/*z* (%): 734 $[M + 1]^+$. λ_{max} (cm^{-1}) in DMF, 11,695, 12,820, 24,937.

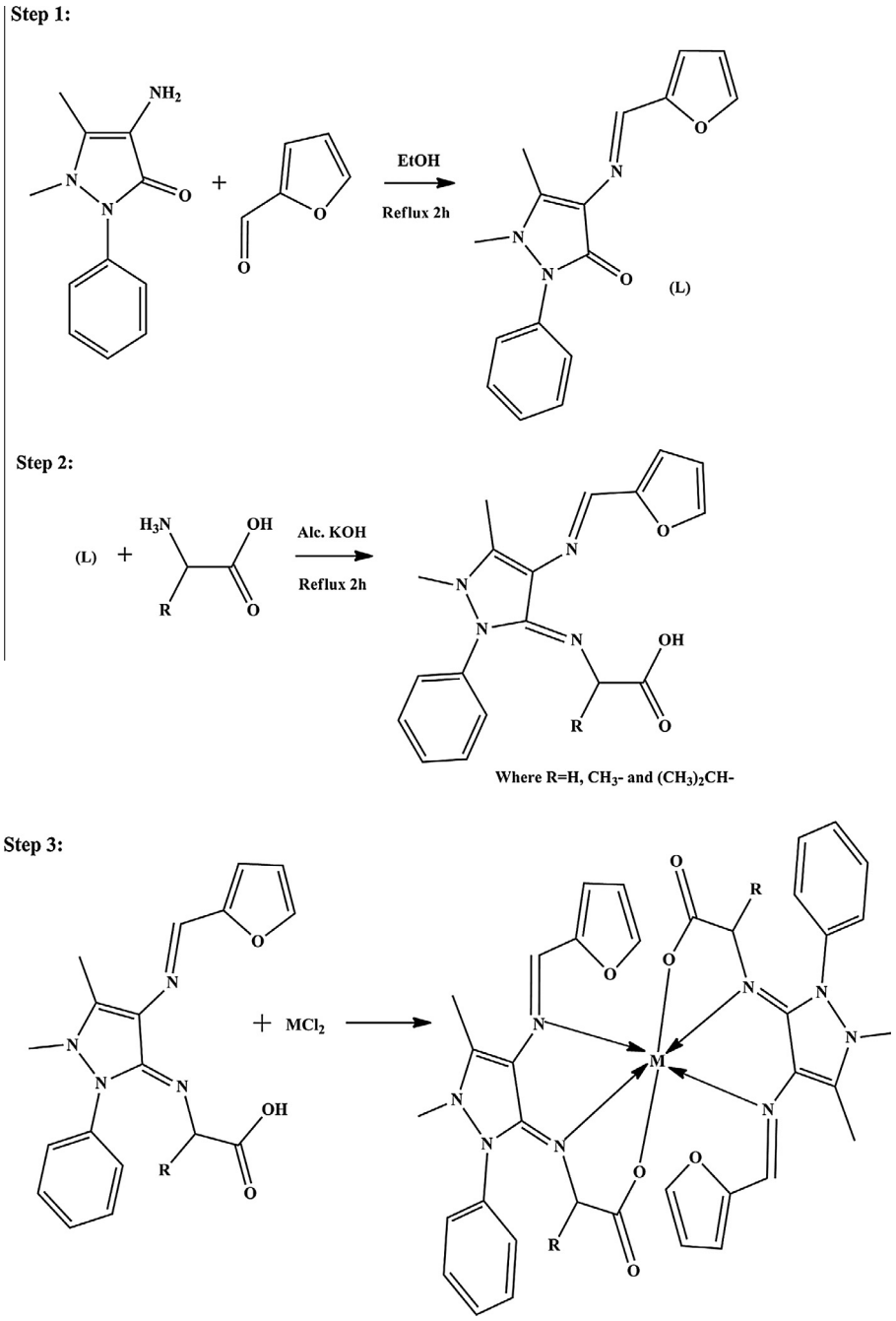

Scheme 1. Schematic route for the synthesis of Schiff base ligands and their metal complexes.

[Ni(L2)$_2$]. Yield: 79%. M.F. $C_{38}H_{38}N_8O_6Ni$. IR (KBr pellet, cm^{-1}): 1637 ν(—C=N); 1595 ν(—HC=N); 1419, 1381 ν((—COO^-) ν_{asy}, (—COO^-) ν_{sy}); 501 ν(M—O); 435 ν(M—N). MS *m*/*z* (%): 762 $[M+1]^+$. λ_{max} (cm^{-1}) in DMF, 11,049, 12,468, 29,411.

[Ni(L3)$_2$]. Yield: 63%. M.F. $C_{42}H_{46}N_8O_6Ni$. IR (KBr pellet, cm^{-1}): 1647 ν(—C=N); 1587 ν(—HC=N); 1415, 1380 ν((—COO^-) ν_{asy}, (—COO^-) ν_{sy}); 584 ν(M—O); 420 ν(M—N). MS *m*/*z* (%): 734 $[M+1]^+$. λ_{max} (cm^{-1}) in DMF, 11,061, 12,642, 29,498.

[Zn(L1)$_2$]. Yield: 72%. M.F. $C_{36}H_{34}N_8O_6Zn$. IR (KBr pellet, cm^{-1}): 1647 ν(—C=N); 1595 ν(—HC=N); 3410, 1411, 1382 ν((—COO^-), (—COO^-) ν_{asy}, (—COO^-) ν_{sy}); 501 ν(M—O); 433 ν(M—N). ^{1}H NMR (δ): (aromatic) 6.6–7.1 (m); (C—CH_3) 2.3 (s); (N—CH_3) 3.1(s); (CH=N) 9.6(s). MS *m*/*z* (%): 741 $[M+1]^+$. λ_{max} (cm^{-1}) in DMF, 29,411, 35,842.

[Zn(L2)$_2$]. Yield: 72%. M.F. $C_{38}H_{38}N_8O_6Zn$. IR (KBr pellet, cm^{-1}): 1647 ν(—C=N); 1597 ν(—HC=N); 1419, 1381 ν((—COO^-) ν_{asy}, (—COO^-) ν_{sy}); 501 ν(M—O); 435 ν(M—N). ^{1}H NMR (δ): (aromatic) 6.6–7.3 (m); (C—CH_3) 2.3 (s); (N—CH_3) 3.1(s); (CH=N) 9.6(s). MS *m*/*z* (%): 769 $[M+1]^+$. λ_{max} (cm^{-1}) in DMF, 29,498, 35,460.

[Zn(L3)$_2$]. Yield: 82%. M.F. $C_{42}H_{46}N_8O_6Zn$. IR (KBr pellet, cm^{-1}): 1645 ν(—C=N); 1587 ν(—HC=N); 1416, 1386 ν((—COO^-) ν_{asy}, (—COO^-) ν_{sy}); 542 ν(M—O); 420 ν(M—N). ^{1}H NMR (δ): (aromatic) 6.6–7.4 (m); (C—CH_3) 2.3 (s); (N—CH_3) 3.1(s); (CH=N) 9.6(s). MS *m*/*z* (%): 825 $[M+1]^+$. λ_{max} (cm^{-1}) in DMF, 29,325, 35,971.

DNA binding experiments

The interaction between metal complexes and DNA was studied by electronic absorption, viscosity and electrochemical methods. Disodium salt of calf thymus DNA was stored at 4 °C. All the experiments involving the interaction of the complexes with calf thymus (CT) DNA were carried out in Tris–HCl buffer (50 mM Tris–HCl, pH 7.2) containing 5% DMF at room temperature. Solution of CT DNA in the buffer gave a ratio of UV absorbance at 260 and 280 nm, A_{260}/A_{280} of *ca*1.89:1, indicating that the CT DNA was sufficiently free from protein [8]. The concentration of DNA was measured by using its extinction coefficient at 260 nm (6600 $M^{-1}cm^{-1}$) after 1:100 dilution. Stock solutions were stored at 4 °C and used not more than 4 days. Doubly distilled water was used to prepare solutions. Concentrated stock solutions of the complexes were prepared by dissolving the complexes in DMF and diluting properly with the corresponding buffer to the required concentration for all the experiments.

The electronic spectra of the complexes were recorded before and after the addition of DNA in the presence of 5 mM Tris–HCl/50 mM NaCl buffer (pH 7.2). The intrinsic binding constant for the interaction of complex with DNA was obtained from absorption data. A fixed concentration value of complex (10 μM) was titrated with increasing amounts of DNA over the range of 20–150 μM. The equilibrium binding constant (K_b) values for the interaction of the complexes with DNA were obtained from the absorption spectral titration data using the following equation:

$$[DNA]/(\varepsilon_a - \varepsilon_f) = [DNA/(\varepsilon_b - \varepsilon_f)] + 1/K_b(\varepsilon_b - \varepsilon_f)$$

where ε_a the extinction coefficient observed for the charge transfer absorption at a given DNA concentration, ε_f, the extinction coefficient of the complex free in solution, ε_b, the extinction coefficient of the complex when fully bound to DNA, K_b, the intrinsic binding constant and [DNA], the concentration in nucleotides. A plot of $[DNA]/(\varepsilon_a - \varepsilon_f)$ *versus* [DNA], gives K_b as the ratio of the slope to the intercept.

Cyclic voltammetry studies were performed on a CHI 620C electrochemical analyzer with three electrode system of glassy carbon as the working electrode, a platinum wire as auxiliary electrode and Ag/AgCl as the reference electrode. Solutions were deoxygenated by purging with N_2 prior to measurements. Viscosity experiments were carried on an Ostwald viscometer, immersed in a thermostated water-bath maintained at a constant temperature at 30.0 ± 0.1 °C. CT DNA samples of approximately 0.5 mM were prepared by sonicating in order to minimize complexities arising from CT DNA flexibility [9]. Flow time was measured with a digital stopwatch three times for each sample and an average flow time was calculated. Data were presented as $(\eta/\eta_0)^{1/3}$ *versus* the concentration of the metal(II) complexes, where η is the viscosity of CT DNA solution in the presence of complex, and η_0 is the viscosity of CT DNA solution in the absence of complex. Viscosity values were calculated after correcting the flow time of buffer alone (t_0), $\eta = (t - t_0)/t_0$ [10].

Interaction with pUC19 plasmid DNA

The extent of *pUC19* DNA cleavage in presence of activating agent AH_2 (ascorbic acid), and two radical scavengers DMSO (hydroxyl radical scavenger) and NaN_3 (singlet oxygen scavenger) was monitored using agarose gel electrophoresis. In reactions using super coiled *pUC19* plasmid DNA Form I (10 μM) in Tris–HCl buffer (50 mM) with 50 mM NaCl (pH 7.2) which was treated with the metal complex and ascorbic acid (10 μM) followed by dilution with the Tris–HCl buffer to a total volume of 20 μL. The samples were incubated for 1 h at 37 °C. A loading buffer containing 0.25% bromophenol blue was added and electrophoresis was performed at 40 V for each hour in Tris–Acetate-EDTA (TAE) buffer using 1% agarose gel containing 1.0 μg/mL ethidium bromide. The cleavage efficiency was measured by determining the ability of the complex to convert the super coiled (SC) DNA to nicked circular form (NC) and linear form (LC). Inhibition reactions were carried out by prior incubation of the *pUC19* DNA (10 mM) with DMSO (4 μL).

Antimicrobial studies

Antibacterial activity

National Committee for Clinical Laboratory Standard (NCCLS) approved standard nutrient agar was used as medium for testing the activity of microorganisms as antibacterial agents [11]. For preparing the agar media, 3 g of beef extract, 5 g of peptone, 5 g of yeast extract and 5 g of sodium chloride were dissolved in 1000 mL of distilled water in a clean conical flask. The pH of the solution was maintained at 7. The solution was boiled to dissolve the medium completely and sterilized by autoclaving at 15 lbs pressure (120 °C) for 30 min. After sterilization, 20 mL of media was poured into the sterilized petri plates. These petri plates were kept at room temperature for sometime. After few minutes the medium got solidified in the plates. Then, it was inoculated with microorganisms using sterile swabs. The stock solutions were prepared by dissolving the compounds in appropriate solvents.

In a typical procedure [8], the antibacterial activities of the compounds were evaluated by the disc diffusion method against the bacterial microorganisms. The 5 mm diameter and 1 mm thickness of the disc was filled with the test solutions using a micropipette and the plates were incubated at 37 °C for 24 h. During this period, the test solution was diffused and affected the growth of the inoculated bacteria. The zone of inhibition, developed on the plate was measured.

Antifungal activity

NCCLS approved standard potato dextrose agar was used as medium for antifungal activity by disc diffusion method [8]. For preparing the agar media, 200 g of potato extract, 20 g of agar and 20 g of dextrose were dissolved in 1000 mL of distilled water in a clean conical flask. The solution was boiled to dissolve the medium completely and sterilized by autoclaving at 15 lbs pressure (120 °C) for 30 min. After sterilization, 20 mL of media was poured into the sterilized petri plates. These petri plates were kept at room temperature for sometime. After few minutes the medium got solidified in the plates. Then, it was inoculated with microorganisms using sterile swabs. In a typical procedure [8], the antifungal activities of the compounds were evaluated by the disc diffusion method against the fungal microorganisms. The 5 mm diameter and 1 mm thickness of the disc was filled with the test solution using a micropipette and the plates were incubated at 37 °C for 72 h. During this period, the test solution was diffused and affected the growth of the inoculated fungi. After 36 h of incubation at 37 °C, the diameter of the inhibition was measured. Compounds showing promising antibacterial/antifungal activity were selected for minimum inhibitory concentration studies. The minimum inhibitory concentration was determined by assaying at concentration of compounds along with standards at the same concentration. Minimum inhibitory concentration (MIC) is the lowest concentration of an antimicrobial compound, inhibiting the visible growth of microorganisms after overnight incubation. Minimum inhibitory concentrations are important in diagnostic laboratories to confirm resistance of microorganisms to antimicrobial agents and also to monitor the activity of new antimicrobial agents.

Antioxidant property

Hydroxyl radicals were generated in aqueous media through the Fenton-type reaction [12,13]. The aliquots of reaction mixture (3 mL) contained 1.0 mL of 0.10 mmol aqueous safranin, 1 mL of 1.0 mmol aqueous EDTA–Fe(II), 1 mL of 3% aqueous H_2O_2, and a series of quantitative microaddition of solutions of the test compound. A sample without the tested compound was used as the control. The reaction mixtures were incubated at 37 °C for 30 min in a water bath. The absorbance was then measured at 520 nm. All the tests were run in triplicate and are expressed as the mean and standard deviation (SD) [14]. The scavenging effect for $OH^{\cdot}$ was calculated from the following expression:

$$\text{Scavenging ratio } (\%) = [(A_i - A_o)/(A_c - A_o)] \times 100\%$$

where A_i is the absorbance in the presence of the test compound; A_o is the absorbance of the blank in the absence of the test compound; A_c is the absorbance in the absence of the test compound, EDTA–Fe(II) and H_2O_2.

Results and discussion

The Schiff base ligands (L1), (L2) and (L3) and their Co(II), Cu(II), Ni(II) and Zn(II) complexes have been synthesized and characterized by spectral and elemental analysis data. The complexes are found to be air stable. The ligands are soluble in common organic solvents and all the complexes are freely soluble in $CHCl_3$, DMF and DMSO.

Elemental analysis and molar conductivity measurements

The results of elemental analysis for the metal complexes are in good agreement with the calculated values (Table 1) showing that the complexes have 1:2 metal–ligand stoichiometry of the type $M(L)_2$ wherein L acts as a tridentate ligand. The metal(II) complexes were dissolved in DMF and the molar conductivities of 10^{-3} M of their solution at room temperature were measured. The lower conductance values (18–34 $ohm^{-1}\ cm^{-2}\ mol^{-1}$) of the complexes support their non-electrolytic nature.

Mass spectra

The mass spectrum of Schiff base ligand (L1) shows the molecular ion peak at *m/z* 338 corresponding to $[C_{18}H_{17}N_4O_3]^{+\cdot}$ ion. Also the spectrum exhibits peaks for the fragments at *m/z* 294, 280, 265, 236 and 156 corresponding to $[C_{17}H_{17}ON_4]^{+\cdot}$, $[C_{16}H_{15}N_4O]^{+\cdot}$, $[C_{15}H_{12}ON_4]^{+\cdot}$, $[C_{14}H_9ON_3]^{+\cdot}$ and $[C_9H_5N_3]^{+\cdot}$ respectively. The spectrum of $[Cu(L1)_2]^{+\cdot}$ complex shows molecular ion peak at *m/z* 739[M + 1] which is equivalent to its molecular weight. The $[Cu(L1)_2]$ complex gives fragment ion peaks at *m/z* 681, 617, 537, 508, 493 and 416 corresponding to $[C_{34}H_{32}N_8O_4Cu]^{+\cdot}$, $[C_{34}H_{32}N_8O_4]^{+\cdot}$, $[C_{29}H_{28}N_8O_3]^{+\cdot}$, $[C_{28}H_{25}N_7O_3]^{+\cdot}$, $[C_{27}H_{22}N_7O_3]^{+\cdot}$ and $[C_{21}H_{17}N_7O_3]^{+\cdot}$ ions respectively. The mass spectrum of Schiff base ligand (L2) shows molecular ion peak at *m/z* 352 for $[C_{19}H_{19}N_4O_3]^{+\cdot}$ and its Co(II) complex shows molecular ion peak at *m/z* 763 [M + 1] for the ion $[CoC_{38}H_{38}N_8O_6]^{+\cdot}$ and its fragmentation peaks at *m/z* are 704, 646, 566, 537, 522, 444 and 363 corresponding to $[C_{38}H_{38}N_8O_6]^{+\cdot}$, $[C_{36}H_{36}N_8O_4]^{+\cdot}$, $[C_{31}H_{32}N_8O_3]^{+\cdot}$, $[C_{30}H_{29}N_7O_3]^{+\cdot}$, $[C_{29}H_{26}N_7O_3]^{+\cdot}$, $[C_{23}H_{21}N_7O_3]^{+\cdot}$, and $[C_{18}H_{17}N_7O_2]^{+\cdot}$ ions respectively. In the similar manner the mass spectrum of Schiff base ligand (L3) shows the molecular ion peak at *m/z* 380 corresponding to $[C_{21}H_{23}N_4O_3]^{+\cdot}$ ion and also the spectrum exhibits peaks for the fragments at *m/z* 365, 288, 209 corresponding to $[C_{20}H_{20}N_4O_3]^{+\cdot}$, $[C_{14}H_{15}N_4O_3]^{+\cdot}$ and $[C_9H_{11}N_4O_2]^{+\cdot}$ ions respectively. The spectrum of $[Zn(L3)_2]^{+\cdot}$ complex shows molecular ion peak at *m/z* 825 [M + 1] which is equivalent to its molecular weight. The *m/z* values of all the fragments of the ligands and their complexes confirm the stoichiometry of the complexes as $[ML_2]$.

Infrared spectra of the ligands and their metal complexes

The coordination mode and sites of the ligands to the metal ions were investigated by comparing the infrared spectra of the free ligands with their metal complexes. The IR spectra of the Schiff base ligands (L1, L2 and L3) show a band at 1602 cm^{-1} which is assigned to azomethine $\nu_{(CH=N)}$ linkage, originating from amino and carbonyl groups of the starting reagents (4-aminoantipyrine and furfural). These bands are shifted towards lower frequencies in the spectra of their metal complexes (1587–1597 cm^{-1}). The comparison of the IR spectra of the complexes with the above Schiff bases indicates the involvement of the azomethine nitrogen in chelation with the metal ion. The coordination of nitrogen to the metal ion could be expected to reduce the electron density of the azomethine link and thus causes a shift in the $\nu_{(CH=N)}$ group. In addition, the ligand also exhibits a band at 1652 cm^{-1} due to the $\nu_{(C=N)}$ vibration, originating from the condensation of amino group of amino acid (glycine, alanine and valine) and furfurlyidine-4-aminoantipyrine which is shifted by 13 cm^{-1} on complexation. Moreover, the coordination of the ligand to the metal centre *via* the carboxylic group can also be obvious from the difference of maxima positions as observed for $\upsilon_{sy(COO^-)}$ and $\upsilon_{asy(COO^-)}$. The bands are observed at 1390 and 1427 cm^{-1} respectively, for a free ligand. For comparison, the $\upsilon_{sy(COO^-)}$ and $\upsilon_{asy(COO^-)}$ are displayed at 1363–1389 and

Table 1
Analytical and physical data of Schiff base ligands and their metal complexes.

S.No	Compound	Found (calc)%				Λ_m (mho $cm^2\ mol^{-1}$)	Magnetic moment (BM)
		M	C	H	N		
1	L1	–	63.9 (64.1)	4.9 (5.1)	16.5 (16.6)	–	–
2	$[Cu(L3)_2]$	7.8 (7.9)	53.3 (53.4)	4.1 (4.2)	13.2 (13.9)	23.4	1.87
3	$[Co(L3)_2]$	7.3 (7.3)	53.6 (53.7)	4.1 (4.3)	13.8 (13.9)	18.8	4.94
4	$[Ni(L3)_2]$	7.2 (7.3)	53.6 (53.8)	4.1 (4.3)	13.9 (13.9)	29.4	3.08
5	$[Zn(L3)_2]$	7.9 (8.1)	53.3 (53.3)	4.1 (4.2)	13.7 (13.8)	21.1	Diamagnetic
6	L2	–	64.8 (64.9)	5.4 (5.5)	15.8 (15.9)	–	–
7	$[Cu(L2)_2]$	7.4 (7.6)	54.6 (54.5)	4.5 (4.6)	13.2 (13.4)	18.0	1.85
8	$[Co(L2)_2]$	6.9 (7.1)	54.7 (54.8)	4.5 (4.6)	13.4 (13.5)	19.1	4.83
9	$[Ni(L2)_2]$	6.9 (7.1)	54.8 (54.8)	4.5 (4.6)	13.3 (13.5)	32.4	3.16
10	$[Zn(L2)_2]$	7.7 (7.8)	54.4 (54.7)	4.5 (4.6)	13.3 (13.4)	20.9	Diamagnetic
11	L3	–	66.3 (66.5)	6.1 (6.1)	14.7 (14.8)	–	–
12	$[Cu(L3)_2]$	7.1 (7.1)	56.4 (56.5)	5.1 (5.2)	12.5 (12.5)	34.0	1.86
13	$[Co(L3)_2]$	6.5 (6.6)	56.6 (56.8)	5.2 (5.2)	12.5 (12.6)	31.5	4.91
14	$[Ni(L3)_2]$	6.5 (6.6)	56.7 (56.8)	5.1 (5.2)	12.5 (12.6)	26.5	3.07
15	$[Zn(L3)_2]$	7.2 (7.3)	56.2 (56.4)	5.1 (5.2)	12.4 (12.5)	28.6	Diamagnetic

1409–1419 cm^{-1}, respectively for all the metal complexes. These results reveal that the organic ligand is involved in the coordination through the carboxyl group. Conclusive evidence of the bonding is also shown by the observation that new bands in the spectra of all metal complexes appearing in the low frequency regions at 500–584 cm^{-1} and 420–449 cm^{-1} characteristic to υ(M—O) and υ(M—N) stretching vibrations respectively, that are not observed in the spectra of free ligands.

^{1}H NMR spectra

The ^{1}H NMR spectra of the Schiff bases (L1), (L2) and (L3) and their zinc complexes were recorded at room temperature in $CDCl_3$. The ^{1}H NMR spectra of ligand (L1) and its $[Zn(L1)_2]Cl_2$ are given in Figs. S1a and S1b (Supplementary file). ^{1}H NMR spectrum of the Schiff base ligand shows peaks at 6.6–7.4 δ which are attributed to phenyl multiplet of Schiff base ligand (obtained from the condensation of 4-aminoantipyrine and furfuraldehyde). The ligand also shows the following signals: C—CH_3 2.3–2.4 δ(s), N—CH_3 3.1–3.3 δ(s); CH=N 9.3 δ(s) and 6.62, 6.94 and 7.83 δ for furfurylidene moiety. The azomethine proton —CH=N signals in the spectra of the zinc complexes are shifted to down field (9.6 δ) compared to the free ligands, suggesting deshielding of azomethine group due to the coordination with metal ion. There is no appreciable change in all other signals of the complexes. The peak at 11 δ is attributed to the —COOH of amino acid (glycine/alanine/valine) moiety present in Schiff bases. The absence of this peak noted for the zinc(II) complexes confirms the loss of the COOH proton of amino acid moiety due to complexation.

Magnetic moments and electronic spectra

The free Schiff base ligands (L1/L2/L3) exhibit two intense bands in 29,240 & 37,075 (L1), 29,411 & 35,335 (L2) and 29,450 & 35,575 cm^{-1} (L3) which are due to π–π* and n–π* transitions respectively. In all metal complexes, the absorption bands are observed in the regions 35,842–37,453 and 29,375–29,761 cm^{-1} which are due to π–π* and n–π* transitions. These transitions exhibit blue or red shift due to the coordination of the ligand with metal ions. The electronic spectra of $[Cu(L1)_2]$, $[Cu(L2)_2]$ and $[Cu(L3)_2]$ complexes exhibit one broad band at 11,050, 11,049 and 12,254 cm^{-1} respectively with low intensity hump which is assigned to $^2E_g \rightarrow {}^2T_{2g}$ transition. The above data reveal that the Cu(II) complexes adopt distorted octahedral geometry around the central metal ion. The observed magnetic moments of the complexes (1.87, 1.85 and 1.86 BM respectively) at room temperature indicate the non-coupled mononuclear complexes of magnetically diluted d^9 system with $s = 1/2$ spin state of distorted octahedral geometry [15]. The monomeric nature of the complexes is further supported by micro analytical and mass spectral data. The electronic spectra of $[Co(L1)_2]$, $[Co(L2)_2]$ and $[Co(L3)_2]$ complexes show three broad bands in the regions 11,025, 14,903, 29,280, 12,150, 13,774, 29,325 and 11,049, 12,500, 29,761 cm^{-1} respectively which are assigned to $^4T_{1g}(F) \rightarrow {}^4T_{2g}(F)$, $^4T_{1g}(F) \rightarrow {}^4A_{2g}(F)$ and $^4T_{1g}(F) \rightarrow {}^4T_{2g}(P)$. These data reveal that complexes have octahedral geometry. The observed magnetic moments of cobalt(II) complexes (4.94, 4.83 and 4.91 BM) at room temperature indicate the monomeric nature of the complexes. It is further supported by micro analytical data. The electronic spectra of $[Ni(L1)_2]$, $[Ni(L2)_2]$ and $[Ni(L3)_2]$ complexes show three bands of low intensity in the visible region around 11,695, 12,820 and 24,937 cm^{-1}, 11,049, 12,468 and 29,411 cm^{-1} and 11,061, 12,642, and 29,498 cm^{-1} which are assigned to $^3A_{2g}(F) \rightarrow {}^3T_{2g}(F)$, $^3A_{2g}(F) \rightarrow {}^3T_{1g}(F)$ and $^3A_{2g}(F) \rightarrow {}^3T_{1g}(P)$ transitions respectively suggesting an octahedral geometry around Ni(II) ion. The observed magnetic moments of Ni(II) complexes (3.08, 3.16 and 3.07 BM respectively) at room temperature indicate the non-coupled mononuclear complexes of diluted d^8 system with $s = 1$ spin state of octahedral geometry [16,17]. Monomeric nature of nickel complexes is further proved by their micro analytical data. The electronic absorption spectra of the diamagnetic $[Zn(L1)_2]$, $[Zn(L2)_2]$ and $[Zn(L3)_2]$ show that the bands at 29,411, 35,842, 29,498, 35,460, 29,325 and 35,971 cm^{-1} are assigned to intraligand charge transfer transitions [18].

EPR spectra

EPR studies of paramagnetic transition metal(II) complexes yield information about the distribution of the unpaired electrons and hence about the nature of the bonding between the metal ion and its ligands. The X-band EPR spectra of all copper(II) complexes were recorded in DMSO at liquid nitrogen temperature and at room temperature. The spin Hamiltonian parameters of the complexes have been calculated and summarized in Table 2. The EPR spectra of the copper(II) complexes at room temperature show one intense absorption band in the high field and is isotropic due to the tumbling motion of the molecules [19]. However, these complexes at liquid nitrogen temperature show three well-resolved peaks with low intensities in the low field region (Fig. S2) and one intense peak in the high field region. From this spectral data, it is found that $A_{||}$ 150 for $[Cu(L1)_2]$, 150 for $[Cu(L2)_2]$ and 160 for $[Cu(L3)_2] > A_{\perp}$105 for $[Cu(L1)_2]$, 90 for $[Cu(L2)_2]$ and 85 for $[Cu(L3)_2]$, $g_{||}$ (2.3407, 2.3051 and 2.3147 for $[Cu(L1)_2]$, $[Cu(L2)_2]$ and $[Cu(L3)_2]$) > $g_{\perp}$ (2.0601, 2.0472 and 2.0591 for [$[Cu(L1)_2]$, $[Cu(L1)_2]$ and $[Cu(L3)_2]$) > 2.0027, In all the three, $g_{||}$ and $g_{\perp}$ values are greater than 2.04, consistent with copper(II) in axial symmetry with all the principal axes aligned parallel. These g values indicate an elongated tetragonally distorted octahedral stereochemistry [20]. From the values of g factors, it is determined the geometric parameter G, representing a measure of exchange interaction between Cu(II) centres in polycrystalline compound, using the formula [21]

$$G = g_{||} - 2.0027/g_{\perp} - 2.0027$$

If $G < 4$, it is considered the existence of some exchange interaction between Cu(II) centres and if $G > 4$, the exchange interaction is negligible. The present copper complexes have G values greater than 4 indicating exchange interaction is either absent or very little in the solid complexes. The empirical ratio of $g_{||}/A_{||}$ is frequently used to evaluate distortion in copper(II) complexes. If this ratio is close to 100, it indicates roughly a square-planar structure around the copper(II) ion and the values from 170 to 250 are indicative of distorted tetrahedral geometry. If the ratio is in between 110 and 170, it indicates nearly an octahedral environment around copper(II) ion with small distortion [22]. For the present copper complexes, the $g_{||}/A_{||}$ values are 156, 153 and 144 cm^{-1} which indicate that all the three complexes have distorted octahedral geometry.

The covalency parameters α^2 (covalent in-plane σ-bonding) and β^2 (covalent in-plane π-bonding) have been calculated using the following equations. If $\alpha^2 = 1.0$, it indicates complete ionic character whereas $\alpha^2 = 0.5$ denotes 100% covalent bonding, with assumption of negligible small values of the overlap integral.

$$\alpha^2 = (A_{||}/0.036) + (g_{||} - 2.0027) + 3/7(g_{\perp} - 2.0027) + 0.04$$

$$\beta^2 = (g_{||} - 2.0027)E/(-8\lambda\alpha^2)$$

$$\gamma^2 = (g_{\perp} - 2.0027)E/(-2\lambda\alpha^2)$$

where $\lambda = -828$ cm^{-1} for free copper ion and E is electronic transition energy. From Table 1, the observed β^2 (0.7732) and γ^2 (0.5214) values for $[Cu(L1)_2]$, β^2 (0.6730) and γ^2 (0.3923) values for $[Cu(L2)_2]$ and for $[Cu(L3)_2]$ β^2(0.7804) and γ^2 (0.5682) indicate that there is

Table 2
The spin Hamiltonian parameters of the copper complexes in DMSO solution at 300 and 77 K.

Complex	$A_{\|}$	$A_{\perp}$	A_{iso}	$g_{\|}$	$g_{\perp}$	g_{iso}	G	$g_{\|}/g_{\perp}$	α^2	β^2	γ^2	$K_{\|}^2$	$K_{\perp}^2$
$[Cu(L1)_2]$	150	105	120	2.3407	2.0601	2.1536	5.9931	156	0.8186	0.7732	0.5214	0.6329	0.4268
$[Cu(L2)_2]$	150	90	110	2.3051	2.0472	2.1351	6.8614	153	0.7775	0.6730	0.3923	0.5233	0.0763
$[Cu(L3)_2]$	160	85	110	2.3147	2.0591	2.1448	5.4938	144	0.8202	0.7804	0.5682	0.6401	0.1165

interaction in the out-of-plane π-bonding whereas the in-plane π-bonding is completely ionic. This is further confirmed by orbital reduction factors which are estimated using the following relations: Hathaway [22] pointed out that for pure σ-bonding, $K_{\|} \approx K_{\perp}$ and for in-plane π-bonding $K_{\|} < K_{\perp}$, while for out-of-plane π-bonding $K_{\perp} < K_{\|}$ the following simplified expressions were used to calculate $K_{\|}$ and $K_{\perp}$:

$$K_{\|} = (g_{\|} - 2.0027)E/8\lambda_0$$

$$K_{\perp} = (g_{\perp} - 2.0027)E/2\lambda_0$$

The observed $K_{\|}$ values are (0.6329. 0.5233 and 0.6401) greater than the values of $K_{\perp}$ (0.4268, 0.0763 and 0.1165) implying a greater contribution from out-of-plane π-bonding than from in-plane π-bonding in metal ligand π-bonding.

Thus, the EPR study of the copper(II) complex has provided supportive evidence to the conclusion obtained on the basis of electronic spectrum and magnetic moment value.

DNA binding studies

Absorption titration

There has been an increasing focus on the interaction between DNA and other molecules which is hopeful to understand the action mechanism of some DNA-targeted drugs and toxic agents as well as the origin of few diseases like gene mutation [23]. The binding behavior of the metal complexes to DNA helix is often investigated using absorption spectral titration followed by the changes in the absorbance and shift in the wavelength. The representative absorption spectra of $[Cu(L3)_2]$, $[Zn(L2)_2]$ and $[Cu(L1)_2]$ complexes in the presence and absence of CT-DNA are shown in Figs. S3a–c.The binding mode of complexes to CT-DNA helix has been followed through absorption spectral titrations. With increasing concentration of CT-DNA the absorption bands of the complexes are affected resulting in the tendency of hypochromism and a minor red shift is observed in all the complexes.

Hyperchromic effect and hypochromic effect are the spectral features of DNA concerning its double helix structure. Hypochromism results from the contraction of DNA in the helix axis as well as from the change in conformation on DNA while hyperchromism results from the damage of the DNA double helix structure [24]. The absorption spectrum of $[Cu(L1)_2]$ complex shows an intensive absorption band at 260.1 nm, $[Cu(L2)_2]$ and $[Cu(L3)_2]$ complexes at 339.4 and 341.6 nm respectively in 5 mM Tris–HCl and 50 mM NaCl buffer solution (pH 7.2). Further the intense absorption bands with maxima of 339.8 nm, 342.0 nm and 257.69 nm for $[Co(L1)_2]$, $[Co(L2)_2]$ and $[Co(L3)_2]$, 339.4 nm, 339.0 nm and 340.0 nm for $[Ni(L1)_2]$, $[Ni(L2)_2]$ and $[Ni(L3)_2]$, 339.8 nm, 341.0 nm and 339.0 nm for $[Zn(L1)_2]$, $[Zn(L2)_2]$ and $[Zn(L3)_2]$ respectively have been obtained. These are due to intra ligand $\pi-\pi^*$ transitions. The increase of the concentration of CT-DNA results in the minor bathochromic shift in the range 0.2–3.0 nm and significant hypochromicity lying in the range 8.33–29.56%. The spectroscopic changes suggest that the complexes show appreciable binding property to the CT-DNA. The K_b values are shown in Table 3.

These results suggest that the interaction of synthesized metal(II) complexes with DNA is a significant weak intercalation

Table 3
Electronic absorption spectral properties of Cu(II), Co(II), Ni(II) and Zn(II) complexes.

No	Compound	λ_{max}		Δλ (nm)	H%[a]	K_b (M^{-1})[b]
		Free	Bound			
1	$[Cu(L1)_2]$	260.1	260.9	0.8	20.66	5.520×10^3
2	$[Co(L1)_2]$	339.8	339.6	0.2	13.47	6.600×10^2
3	$[Ni(L1)_2]$	339.4	337.4	2.0	15.3	1.438×10^4
4	$[Zn(L1)_2]$	339.8	339.4	0.4	8.33	1.029×10^5
5	$[Cu(L2)_2]$	339.4	337.02	2.38	20.97	5.570×10^3
6	$[Co(L2)_2]$	342.0	340.0	2.00	11.97	5.813×10^4
7	$[Ni(L2)_2]$	339.0	341.0	2.00	12.73	7.039×10^4
8	$[Zn(L2)_2]$	341.0	339.0	2.00	10.24	5.969×10^4
9	$[Cu(L3)_2]$	341.6	339.6	2.0	28.20	4.181×10^5
10	$[Co(L3)_2]$	257.7	259.3	1.6	21.71	1.113×10^5
11	$[Ni(L3)_2]$	340.0	339.2	0.8	29.56	4.527×10^5
12	$[Zn(L3)_2]$	339.0	342.0	3.0	10.25	6.248×10^4

[a] $H\% = [A_{free} - A_{bound})/A_{free}] \times 100\%$.
[b] K_b = Intrinsic DNA binding constant determined from the UV–Vis absorption spectral titration.

binding mode. From the binding constant values (K_b), it is understood that the valine Schiff-base complexes have more intercalating ability than alanine and glycine Schiff-base complexes. In addition to this, nickel, copper and cobalt complexes are having higher binding constant values than and zinc complexes. In this study, for glycine Schiff base complexes, the OD is increased when DNA is added to the complexes i.e. hyperchromism is observed, which indicates that added complexes break the secondary structure of the DNA during binding. In general binding constant (K_b) values of these synthesized complexes are lower in comparison to those observed for typical intercalators, ethidium bromide and $[Ru(bpy)_2(dppz)]^{2+}$ whose binding constants are in the order of 1.4×10^6 and $>10^6$ M^{-1} [25,26].

Viscosity measurements

The viscometric measurement is also an important tool to find the nature of binding of metal complexes to the DNA. The relative specific viscosity of DNA is determined by varying the concentration of the added metal complexes. In the absence of crystallographic structural data, hydrodynamic methods that are sensitive to DNA length change are regarded as the least ambiguous and the most critical tests of binding in solution. A classical intercalation model results in the lengthening of the DNA helix as the base pairs is separated to accommodate the binding molecule, leading to an increase in the DNA viscosity. However, a partial and non-classical intercalation of ligand may bend (or kink) DNA helix, resulting in the decrease of its effective length and concomitantly its viscosity [27]. The plots of $(\eta/\eta_o)^{1/3}$ *versus* R, (where R = [Complex]/[DNA]; η and η_o are the relative viscosities of DNA in the presence and absence of complex, respectively) give a measure of the viscosity changes. The effects of all the complexes on the viscosity of CT-DNA are shown in Fig. S4. As expected, the known DNA-intercalator ethidium bromide increases the relative viscosity of DNA double helix resulting from intercalation. In contrast, groove (or) surface binding can cause an increase in the effective length of DNA leading to a minor increase in the effective length of DNA solution [28]. All the complexes exhibit minor increase in the relative viscosity of CT-DNA compared to ethidium bromide suggesting primarily groove binding nature of the complexes.

Electrochemical studies

Cyclic and differential pulse voltammetric techniques are extremely useful in probing the nature and mode of DNA binding of metal complexes. Typical cyclic voltammogram of complex, $[Cu(L3)_2]$ in the absence and in the presence of varying amount of [DNA] is shown in Fig. S5a. The incremental addition of CT-DNA to the complex causes decrease of anodic and cathodic peak current of the complex. This result shows that complex stabilizes the duplex (GC pairs) by intercalating way. The incremental addition of CT-DNA to the complex causes shift in the potential of peak in cyclic voltammogram. Both the cathodic and anodic peak show positive or negative shift which indicates intercalation of complex to DNA of base pairs. If one of the shifts is positive and another one is negative, it reveals the intercalation and electrostatic binding of the complex to CT-DNA or it may break the secondary structure of DNA.

In differential pulse voltammogram of the complex, $[Cu(L3)_2]$ in the absence and presence of varying amount of [DNA] with significant decrease of current intensity (Fig. S5b), the shift in potential is related to the ratio of binding constant by the following equation:

$$E_b - E_f = 0.0591 \log(K_{[red]}/K_{[oxd]})$$

where E_b and E_f are peak potentials of the complex in the bound and free form respectively. In the present study, $[M(L1)_2]$, $[M(L2)_2]$ and $[M(L3)_2]$ complexes show one electron transfer during the redox process and their ip_c/ip_a value is less than unity which indicates the reaction of the complex on the glassy carbon electrode surface is quasi-reversible. Other complexes [Co(II), Ni(II), Mn(II) and Zn(II)] show considerable shift in both cathodic and anodic peak potentials in the presence of incremental addition of CT-DNA.

Most of our synthesized complexes give both the anodic and cathodic peak potential shifts which are either positive or negative (Table 4). It indicates the intercalating mode of DNA binding with glycine/alanine/valine ligand Schiff base complexes. It is interesting to note that valine Schiff base ligand complexes give greater decrease in current intensity than alanine and glycine Schiff base ligand complexes. From this observation, it is concluded that intercalative mode of DNA binding to valine ligand complexes is stronger than ala/gly ligand complexes.

Nucleolytic activity

The study on the cleavage capacity of transition metal complex to DNA is considerably interesting as it can contribute to understanding the toxicity mechanism of them and to develop novel artificial nuclease. DNA cleavage is controlled by relaxation of supercoiled circular form of pUC19 DNA into nicked circular form and linear form. When circular plasmid DNA is conducted by electrophoresis the fastest migration will be observed for the super coiled form (Form I). If one strand is cleaved, the supercoils will relax to produce a slow moving open circular form (Form II). If both strands are cleaved a linear form (Form III) will be generated that migrates in between I and II [29,30].

The ability of the complexes in affecting DNA cleavage has been investigated by gel electrophoresis using super coiled pUC19 DNA in Tris–HCl/50 mM buffer medium. When this experiment is carried out to all the three series of complexes, it has been observed that valine (L3) complexes have little bit higher cleavage abilities than alanine (L2) and glysine (L1) complexes. Among the four valine Schiff base complexes, nickel and copper complexes are having higher cleaving ability. All the complexes are found to exhibit nuclease activity. Fig. S6a shows the result of gel electrophoretic separations of plasmid pUC19 DNA induced by an addition of pUC19 DNA, $[M(L3)_2]$ in presence of AH_2 (ascorbic acid). Under the same conditions, free AH_2 produced no cleavage of pUC19 DNA. All super coiled (Form I) DNA was cleaved to form the mixture of form II and form III with the addition of the complex concentration. These phenomena imply that Cu(II), Co(II), Ni(II) and Zn(II) complexes induce intensively the cleavage of plasmid pUC19 DNA in the presence of AH_2.

In order to clarify the cleavage mechanism of pUC19 DNA introduced by $[M(L3)_2]$, the investigation has been carried out further on adding DMSO (hydroxyl radical scavenger). It is found that no inhibition of DNA cleavage has been observed indicating that hydroxyl radical is not involved in the cleavage process (Fig. S6b). On the other hand, addition of sodium azide (singlet oxygen scavenger) does not show any apparent inhibition in the DNA which reveals that the singlet oxygen $^1O_2$ is not responsible for the cleavage reaction (Fig. S6c). These observations suggest that all the complexes mediated cleavage reaction do not proceed *via* radical cleavage.

Antimicrobial screening

Antibacterial activity

The Schiff base complexes have provoked wide interest because they possess a diverse spectrum of biological and pharmaceutical activities. The antibacterial activity of the Schiff base ligands and their metal complexes and streptomycin (as a standard compound) were tested against bacteria because bacteria can achieve resistance to antibiotics through biochemical and morphological modifications [31]. The organisms used in the present investigation included *Staphylococcus aureus*, *Pseudomonas aeruginosa*,

Table 4
Electrochemical parameters for the interaction of DNA with metal(II) complexes.

S. No.	Complexes	$E_{1/2}$ (V)[a]		ΔE_p (V)[b]		k[red]/k[oxd]	Ip_c/Ip_a[a]
		Free	Bound	Free	Bound		
1	$[Cu(L1)_2]$	−0.1035	−0.0785	+0.0470	+0.0750	0.8190	0.7782
2	$[Co(L1)_2]$	−0.1760	−0.1615	+0.0360	+0.0312	0.6640	0.5900
3	$[Ni(L1)_2]$	−0.7623	−0.6128	−0.0325	−0.1064	1.0294	0.5432
4	$[Zn(L1)_2]$	+0.1624	+0.1887	+0.0523	+0.0816	0.7321	0.6560
5	$[Cu(L2)_2]$	−0.1490	−0.1461	−0.0700	−0.0910	0.4980	0.9312
6	$[Co(L2)_2]$	−0.2065	−0.2265	+0.0756	+0.0656	0.1841	0.5260
7	$[Ni(L2)_2]$	−0.1347	−0.1166	−0.0647	−0.0626	0.7589	0.8534
8	$[Zn(L2)_2]$	−0.4923	−0.4320	+0.0670	−0.0220	0.8357	1.0116
9	$[Cu(L3)_2]$	−0.6267	−0.4882	−0.2298	−0.3185	1.0115	0.8619
10	$[Co(L3)_2]$	−0.5035	−0.4810	+0.0620	+0.0230	1.8450	0.9312
11	$[Ni(L3)_2]$	−0.1034	−0.0811	+0.0320	+0.0610	0.8064	0.8126
12	$[Zn(L3)_2]$	−0.1656	−0.1636	+0.0724	+0.0644	0.6816	0.8745

Data from cyclic voltammetric measurements.
[a] $E_{1/2}$ is calculated as the average of anodic (E_{pa}) and cathodic (E_{pc}) peak potentials. $E_{1/2} = E_{Pa} + E_{pc}/2$.
[b] $\Delta E_p = E_{pa} - E_{pc}$.

Table 5
The *in vitro* antibacterial activity of ligands and their metal(II) complexes evaluated by MIC (Minimum Inhibitory Concentration, μg/mL).

Compound	*S. aureus*	*P. aeruginosa*	*E. coli*	*S. epidermidis*	*K. pneumoniae*
L1	20.8	11.9	22.3	24.7	22.4
$[Cu(L1)_2]$	8.8	9.0	3.6	6.4	6.4
$[Co(L1)_2]$	7.2	10.2	2.1	8.8	8.8
$[Ni(L1)_2]$	8.6	8.4	1.8	6.4	8.4
$[Zn(L1)_2]$	10.4	32	1.9	6.0	9.2
L2	18.8	9.9	17.3	18.7	21.4
$[Cu(L2)_2]$	6.7	5.6	4.5	5.2	6.8
$[Co(L2)_2]$	5.2	4.0	4.0	5.9	5.3
$[Ni(L2)_2]$	6.0	2.3	2.4	4.4	7.1
$[Zn(L2)_2]$	5.1	4.6	3.8	2.8	8.3
L3	24.8	10.9	23.3	25.7	26.4
$[Cu(L3)_2]$	6.3	4.0	4.8	4.6	5.4
$[Co(L3)_2]$	4.4	2.8	2.0	3.2	6.2
$[Ni(L3)_2]$	5.9	2.4	4.0	3.0	5.1
$[Zn(L3)_2]$	7.1	3.2	2.2	4.0	7.3
Streptomycin[a]	1.7	1.9	1.8	1.3	2.3

[a] Streptomycin is used as the standard.

Escherichia coli, Staphylococcus epidermidis and *Klebsiella pneumoniae*. The disc diffusion method was used to evaluate the antibacterial activity of the synthesized metal complexes. The minimum inhibitory concentration (MIC) was determined by assaying at serial dilution of concentrations along with standards at the same concentration.

The results of the bactericidal study of the synthesized compounds are displayed in Table 5. All the complexes are more potent than the ligand towards the specified bacteria species. Moreover, all the glysine Schiff base complexes are having higher antimicrobial activities than alanine and valine complexes. As the number of alkyl group in the ligand increases, it will decrease antibactericidal activity of the complexes. The remarkable activity of the Schiff base ligand may be due to the presence of azomethine group which imports in elucidating the mechanism of transformation reaction in biological system. All the metal complexes are found to have higher antibacterial activity against Schiff base ligands. The antibacterial results evidently show that the activity of the Schiff base compounds becomes more pronounced when coordinated to the metal ions. The studies reveal that a significant antibacterial activity can be induced for complexes by using either a biocation or a metallic ion exhibiting inhibitory properties as well as a ligand that displays such activity. This enhancement in the activity may be rationalized on the basis that their structures mainly possess an additional C=N bond along with azomethine group.

Antifungal activity

To provide a medicinal scope in the field of bioinorganic chemistry, consequently, the metal complexes synthesized have been evaluated for their antifungal actions. The antifungal tests were carried out using the disc diffusion method. The Schiff base ligands and their metal complexes were screened *in vitro* in order to find out the antifungal activity against *Aspergillus niger, Aspergillus flavus, Culvularia lunata, Rhizoctonia bataicola* and *Candida albicans*. The results of the antifungal studies are presented in Table 6 which reveal that the metal complexes are toxic than the free ligands against the same organisms. Moreover, all the glycine complexes are having higher antifungal activities than alanine and valine complexes. As the number of alkyl group in the ligand increases, it will decrease antifungicidal activity of the complexes. The increase in the antifungal activity of the metal complexes inhibits multiplication process of the microbes by blocking their active sites. Such increased activity on metal chelation can be explained on the basis of Tweedy's chelation theory [32]. The chelation also increases the lipophilic nature and the interaction between the metal ion and the lipid is favored. This may lead to the breakdown of the permeability barrier of the cell resulting in interference with the normal cell processes. While chelation is not the only factor for antimicrobial activity, it is an intricate blend of several aspects such as nature of the metal ion and the ligand, the geometry of the metal complexes, the lipophilicity, the presence of co-ligands,

Table 6
The *in vitro* antifungal activity of ligands and their metal(II) complexes evaluated by MIC (Minimum Inhibitory Concentration, μg/mL).

Compound	*Aspergillus niger*	*Aspergillus flavus*	*Culvularia lunata*	*Rhizoctonia bataicola*	*Candida albicans*
L1	22.3	11.4	20.3	22.7	24.4
$[Cu(L1)_2]$	9.4	7.2	5.4	9.3	6.4
$[Co(L1)_2]$	10.2	9.8	4.6	5.4	16.5
$[Ni(L1)_2]$	8.6	4.2	3.3	7.3	6.1
$[Zn(L1)_2]$	8.4	5.3	3.4	7.2	4.9
L2	25.3	8.4	18.3	21.7	26.4
$[Cu(L2)_2]$	11.2	5.9	4.2	5.8	9.3
$[Co(L2)_2]$	9.4	5.6	4.6	5.3	7.8
$[Ni(L2)_2]$	9.1	5.8	5.7	7.0	9.6
$[Zn(L2)_2]$	12.2	6.5	4.5	7.2	10.8
L3	22.3	12.4	21.3	23.7	24.4
$[Cu(L3)_2]$	12.32	5.1	4.1	4.0	10.2
$[Co(L3)_2]$	15.44	4.6	3.3	3.8	11.32
$[Ni(L3)_2]$	13.32	4.6	2.8	3.4	9.35
$[Zn(L3)_2]$	16.25	4.12	3.1	6.4	12.35
Nystatin[a]	1.1	1.7	1.2	1.0	1.5

[a] Nystatin is used as the standard.

the steric and pharmacokinetic factors [33]. The synthesized compounds having amino acid moieties also show good activity.

Antioxidant property

According to relevant reports in the literature [34–37], few transition metal complexes may exhibit antioxidant activity. Hence, it is tried to explore whether the synthesized complexes have the hydroxyl radical scavenging property. The scavenging property of the hydroxyl radicals of the synthesized complexes has been compared to the well-known natural antioxidants mannitol and vitamin C, using the same method as reported by Wu et al. [38]. The 50% inhibitory concentration (IC_{50}) values of mannitol and vitamin C are about 9.6×10^{-3} and $8.7 \times 10^{-3} M^{-1}$ respectively. According to the antioxidant experiments, the IC_{50} values of $[Ni(L1)_2]$ and $[Zn(L1)_2]$ complexes are 1×10^{-7} M^{-1} and 1×10^{-8} M^{-1} respectively which imply that above zinc and nickel complexes have preferable ability to scavenge hydroxyl radical. The antioxidant behavior is also observed in all valine Shiff base ligand complexes. The IC_{50} value of $[Cu(L3)_2]$ complex is 1×10^{-4} M^{-1} .This value also shows that $[Cu(L3)_2]$ complex has preferable ability to scavenge hydroxyl radical. Based on the view of the observed IC_{50} values, the $[Ni(L1)_2]$ and $[Zn(L1)_2]$ complexes can be considered as potential drugs to eliminate the hydroxyl radicals.

Conclusion

This work describes the synthesis and characterization of 4-aminoantipyrine derived Schiff bases and their metal(II) complexes. The Schiff base ligands are behaving as nitrogen and oxygen donor tridentate ligands. The structure of the complexes has been determined on the basis of elemental analyses, molar conductivities, IR spectra, UV–Vis., Mass spectra and ^1H NMR spectra. All these studies give good evidence for the proposed structure. The complexes are shown to act as active DNA binding agents. Binding constants for the above synthesized complexes are found to be in the order of 10^2 to 10^5 indicating that most of the synthesized complexes are good intercalators. Gel electrophoresis experiment shows that presence of ascorbic acid enhances the DNA cleavage to a significant extent. The biological activities of the Schiff bases under investigation and their complexes against bacterial and fungal organisms are promising which need further and deep studies on animals and humans. The antibacterial and antifungal activities of the ligands and their complexes exhibit that the complexes have potent biocidal and fungicidal activity than the free ligands. In antioxidant experiments, the IC_{50} values of $[Ni(L1)_2]$ and $[Zn(L1)_2]$ complexes are 1×10^{-7} M^{-1} and 1×10^{-8} M^{-1} respectively which imply that the above zinc and nickel complexes have preferable ability to scavenge hydroxyl radical. In view of the observed IC_{50} values, the $[Ni(L1)_2]$ and $[Zn(L1)_2]$ complexes can be considered as potential drugs to eliminate the hydroxyl radical.

Acknowledgements

The authors express their sincere thanks to the College Managing Board, Principal and Head of the Department of Chemistry, VHNSN College for providing necessary research facilities. They also thank the Sophisticated Analytical and Instrumentation Facility, Central Drug Research Institute, Lucknow, for providing CHN-analysis data and FAB-Mass spectra and Sophisticated Analytical and Instrumentation Facility, Indian Institute of Technology, Bombay, for EPR measurements.

Appendix A. Supplementary material

Supplementary data associated with this article can be found, in the online version, at http://dx.doi.org/10.1016/j.saa.2014.01.108.

References

[1] S. Chandra, D. Jain, A.K. Sharma, P. Sharma, Molecules 14 (2009) 174–190.
[2] N. Raman, M. Selvaganapathy, Inorg. Chem. Commun. 37 (2013) 114–120.
[3] T. Rosu, M. Negoiu, S. Pasculescu, E. Pahontu, D. Poirier, A. Gulea, Eur. J. Med. Chem. 45 (2010) 774–781.
[4] C. Leelavathy, S. Arul Antony, Spectrochim. Acta 113A (2013) 346–355.
[5] T. Rosu, E. Pahontu, C. Maxim, R. Georgescu, N. Stanica, G.L. Almajan, A. Gulea, Polyhedron 29 (2010) 757–766.
[6] K. Shanker, R. Rohini, K. Shravankumar, P. Muralidhar Reddy, Y.P. Ho, V. Ravinder, Spectrochim. Acta 73A (2009) 205–211.
[7] P. Krishnamoorthy, P. Sathyadevi, A.H. Cowley, R.R. Butorac, N. Dharmaraj, Eur. J. Med. Chem. 46 (2011) 3376–3387.
[8] J. Marmur, J. Mol. Biol. 3 (1961) 208–218.
[9] J.B. Charies, N. Dattagupta, D.M. Crothers, Biochemistry 21 (1982) 3933–3937.
[10] S. Satyanarayanan, J.C. Davorusak, J.B. Charies, Biochemistry (1983) 2573–2584.
[11] J.G. Cappuccino, N. Sherman, Microbiology Lab Manual, fourth ed., 1996.
[12] C.C. Winterbourn, Biochem. J. 198 (1981) 125–131.
[13] C.C. Winterbourn, Biochem. J. 182 (1979) 625–628.
[14] Z.Y. Guo, R.E. Xing, S. Liu, H.H. Yu, P.B. Wang, C.P. Li, P.C. Li, Bioorg. Med. Chem. Lett. 15 (2005) 597–600.
[15] A.B.P. Lever, Inorganic Electronic Spectroscopy, second ed., Elsevier, New York, 1968.
[16] F.A. Cotton, G. Wilkinson, Advanced Inorganic Chemistry, fifth ed., Wiley, New York, 1988.
[17] S.S. Konstantinovic, B.C. Radovanovic, A. Krkljes, J. Therm. Anal. Calorim. 90 (2007) 525–531.
[18] N. Raman, K. Pothiraj, T. Baskaran, J. Mol. Struct. 1000 (2011) 135–328.
[19] R.K. Ray, G.B. Kauffman, Inorg. Chim. Acta 173 (1990) 207–214.
[20] V. Prasad Singh, A. Katiyar, Pestic. Biochem. Phys. 92 (2008) 8–14.
[21] B.J. Hathaway, J.N. Bardley, R.D. Gillard (Eds.), Essays in Chemistry, Academic Press, New York, USA, 1971.
[22] B.J. Hathaway, D.E. Billing, Coord. Chem. Rev. 5 (1970) 143–207.
[23] M. Sonmez, M. Celebi, Y. Yardim, Z. Senturk, Eur. J. Med. Chem. 45 (2010) 4215–4220.
[24] Q.S. Li, P. Yang, H.F. Wang, M.L. Guo, J. Inorg. Biochem. 64 (1996) 181–195.
[25] J.B. Lepecp, C. Paoletti, J. Mol. Biol. 27 (1967) 87–106.
[26] A.E. Friedman, J.C. Chambron, J.P. Sauvage, N.J. Turro, J.K. Barton, J. Am. Chem. Soc. 112 (1990) 4960–4962.
[27] S. Sathyanarayana, J.C. Dabroniak, J.B. Chaires, Biochemistry 31 (1992) 9319–9324.
[28] C. Rajput, R. Rutkaite, L. Swanson, I. Haq, J.A. Thomas, Chem. Eur. J. 12 (2006) 4611–4620.
[29] A.K. Patra, T. Bhowmick, S. Roy, S. Ramakumar, A.R. Chakravarty, Inorg. Chem. 48 (2009) 2932–2943.
[30] Q. Saquib, A.A. Al-Khedhairy, S.A. Alarifi, S. Dutta, S. Dasgupta, J. Musarrat, Intl. J. Biol. Macromol. 47 (2010) 68–75.
[31] G.G. Mohamed, Spectrochim. Acta 64A (2006) 188–194.
[32] R. Ramesh, S. Maheswaran, J. Inorg. Biochem. 96 (2003) 457–462.
[33] M. Thankamony, K. Mohanan, Indian J. Chem. 46A (2007) 247–251.
[34] S.B. Bukhari, S. Memon, M. Mahroof-Tahir, M.I. Bhanger, Spectrochim. Acta 71A (2009) 1901–1906.
[35] F.V. Botelho, J.I. Alvarez-Leite, V.S. Lemos, A.M.C. Pimenta, H.D.R. Calado, T. Matencio, C.T. Miranda, E.C. Pereira-Maia, J. Inorg. Biochem. 101 (2007) 935–1112.
[36] Q. Wang, Z.Y. Yang, G.F. Qi, D.D. Qin, Eur. J. Med. Chem. 44 (2009) 2425–2433.
[37] T.R. Li, Z.Y. Yang, B.D. Wang, D.D. Qin, Eur. J. Med. Chem. 43 (2008) 1688–1695.
[38] Huilu Wu, Jingkun Yuan, Ying Bai, Guolong Pan, Hua Wang, Xingbin Shu, J. Photochem. Photobiol. B: Biol. 107 (2012) 65–72.